Electronic Supporting Information

Modulating Living Crystallization-Driven Self-Assembly Behaviors of Oligo(*p*-phenylene ethynylene)-Containing Block Copolymers and Micellar Stability by Solvent and Corona-Forming Chain Length

Jiucheng Nie,[b,c,#] *Longgang Xia*,[a,#] *Xiaoyu Huang*,[b,c,*] *Guolin Lu*,[b] *Chun Feng*[a,b,*]

[a] Shanghai Key Laboratory of Advanced Polymeric Materials, School of Materials Science and Engineering, East China University of Science and Technology, 130 Meilong Road, Shanghai 200237, People's Republic of China

[b] Key Laboratory of Synthetic and Self-Assembly Chemistry for Organic Functional Molecules, Shanghai Institute of Organic Chemistry, University of Chinese Academy of Sciences, Chinese Academy of Sciences, 345 Lingling Road, Shanghai 200032, People's Republic of China

[c] School of Physical Science & Technology, ShanghaiTech University, 100 Haike Road, Shanghai 201210, People's Republic of China

* To whom correspondence should be addressed, E-mail: cfeng@ecust.edu.cn (Tel: +86-21-54925606), xyhuang@mail.sioc.ac.cn (Tel: +86-21-54925310).

#: These authors contributed equally to this work.

SUPPORTING EXPERIMENTAL DETAILS

Materials

Methanol (≥99.9%, Aladdin) and ethanol (≥99.8%, Aladdin) were used as received for self-assembly experiments. *N*-Isopropylacrylamide (NIPAM, Aladdin, 97%) was recrystallized from *n*-hexane. Copper(I) chloride (CuCl, Aladdin, 99%) was purified by stirring overnight over CH_3CO_2H at room temperature, followed by washing the solid with ethanol, diethyl ether and acetone prior to drying *in vacuo* at 40°C overnight. Tris[2-(dimethylamino)ethyl]amine (Me_6TREN, Aladdin, 97%), tris[(1-benzyl-1H-1,2,3- triazol-4-yl)methyl]amine (TBTA, Aladdin, 97%), ethanol (≥99.8%, Aladdin) and tetrahydrofuran (THF, 99.9%, Aladdin) were used as received. Other reagents not specially mentioned were purchased from Aladdin and used as received. Alkyne-terminated OPE_7, azide-terminated $PNIPAM_{22}$, OPE_7-*b*-$PNIPAM_{22}$ and OPE_7-*b*-$PNIPAM_{47}$ were synthesized and purified in a similar way as described in our previous reports.[1,2]

Instrumentation

^{1}H NMR (400 MHz) analyses were performed on a JEOL JNM-ECZ400 spectrometer in $CDCl_3$ or CD_2Cl_2, tetramethylsilane (TMS) was used as internal standard. Relative molecular weights and molecular weight distributions were measured by conventional gel permeation chromatography (GPC) using a system equipped with a Waters 1515 Isocratic HPLC pump, a Waters 2414 refractive index detector, a Waters 2487 dual λ absorbance detector and a set of Waters Styragel columns (HR3 (500-30,000), HR4 (5,000-600,000) and HR5 (50,000-4,000,000, 7.8×300 mm, particle size: 5 μm). GPC measurements were carried out at 35°C

using THF as eluent with a flow rate of 1.0 mL/min. The system was calibrated with linear polystyrene standards.

Transmission electron microscopy (TEM)

TEM images were obtained by a JEOL JEM-2100 instrument operated at 80 kV. A drop of micellar solution (10 μL) was placed on a Formvar and carbon-coated copper grid for 10 s and then a filter paper touched the edge of drop to absorb most of liquid on the grid. The grid was allowed to dry at room temperature. For each sample, the length distribution of micelles was determined by tracing more than 100 individual micelles, and width distributions were determined by making measurements at least 100 different positions on several micelles and analysis using the ImageJ software program from National Institutes of Health. Values of number-average length (L_n), weight-average length (L_w), number-average width (W_n) and weight-average width (W_w) of micelles were calculated as follows:

$$L_n = \frac{\sum_{i=1}^{N} N_i L_i}{\sum_{i=1}^{N} N_i} \quad (1)$$

$$L_w = \frac{\sum_{i=1}^{N} N_i L_i^2}{\sum_{i}^{N} N_i L_i} \quad (2)$$

$$W_n = \frac{\sum_{i=1}^{N} N_i W_i}{\sum_{i=1}^{N} N_i} \quad (3)$$

$$W_w = \frac{\sum_{i}^{N} N_i W_i^2}{\sum_{i=1}^{N} N_i W_i} \quad (4)$$

where N_i is the number of micelles of length L_i or width W_i, and N is the number of calculated micelles in each sample. The distribution of micellar length or width is characterized by both L_w/L_n or W_n/W_i and the standard deviation of the length distribution σ.

X-ray diffraction (XRD) analysis

XRD measurements were conducted by Philips X'Pert PRO X-ray powder diffractometer with Cu*Kα* (1.541 Å) radiation (40 kV, 40 mA) and samples were exposed at a scan rate of 2θ = 0.0334°/s between 3° and 30°. Samples of OPE_7-*b*-$PNIPAM_8$, OPE_7-*b*-$PNIPAM_{22}$ and OPE_7-*b*-$PNIPAM_{47}$ were prepared by casting corresponding CH_2Cl_2 solution onto a silicon wafer, and allowing them to dry at room temperature, respectively.

Differential scanning calorimetry (DSC)

DSC measurements were carried out with a TA Q200 DSC instrument in N_2 with a heating and cooling rate of 10°C/min. The thermal history of all of samples of alkyne-terminated OPE_7, OPE_7-*b*-$PNIPAM_8$, OPE_7-*b*-$PNIPAM_{22}$ and OPE_7-*b*-$PNIPAM_{47}$ was erased by an initial heating/cooling cycle, followed by slow cooling and a subsequent heating cycle (10°C/min). The data were collected over the 2nd cycle of heating.

Polymer Syntheses

Synthesis of alkyne-terminated OPE_7

Alkyne-terminated OPE_7 was synthesized and purified in the way (**Scheme S1**) as described in our previous report.[1]

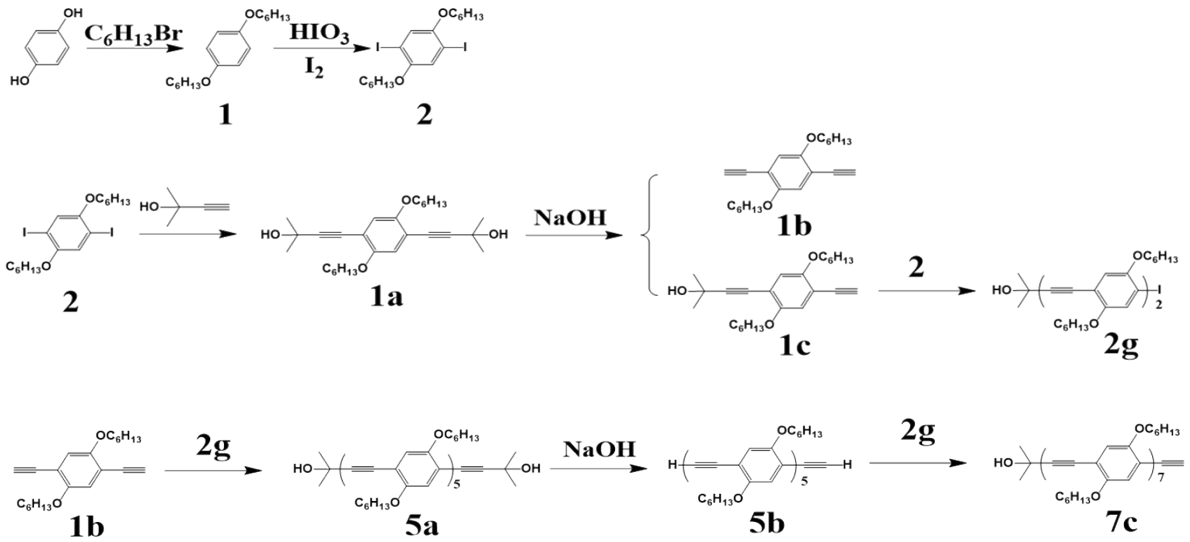

Scheme S1. Synthetic route of alkyne-terminated OPE_7.

5b (200 mg, 0.13 mmol), **2g** (100 mg, 0.13 mmol), $[Pd(PPh_3)_2Cl_2]$ (3 mg, 0.004 mmol) and CuI (1 mg, 0.005 mmol) were added into a 10 mL Schlenk flask, followed by degassing and kept under N_2. Next, THF (2.5 mL) and TEA (2.5 mL) were added via a gastight syringe followed by stirring at room temperature for 5 h. The solvent was evaporated *in vacuo* and the crude product was purified by silica column chromatography (eluent: CH_2Cl_2/petroleum ether = 4/1) to give alkyne-terminated OPE_7-alkyne **7c** (62 mg, 22%) as a yellow solid. MALDI-TOF: calculated $C_{145}H_{204}O_{15}$ for 2187.21; found 2187.0 [M+]. GPC: M_n^{GPC} = 3800 g/mol, M_w/M_n = 1.01. ^{1}H NMR (400 MHz, $CDCl_3$): δ (ppm): 0.87 (m, 42H, $OCH_2CH_2(CH_2)_3CH_3$), 1.33-1.51 (m, 84H, $OCH_2CH_2(CH_2)_3CH_3$), 1.63 (s, 6H, $C(CH_3)_2OH$), 1.84 (m, 28H, $OCH_2CH_2(CH_2)_3CH_3$), 3.34 (s, 1H, alkyne *H*), 4.02 (m, 28H, $OCH_2CH_2(CH_2)_3CH_3$), 6.89-7.00 (m, 14H, Ar*H*).

Synthesis of azide-terminated poly(*N*-isopropylacrylamide)

Azide-terminated $PNIPAM_8$ and $PNIPAM_{22}$ samples were synthesized and purified in the way (**Scheme S2**) as described in our previous reports.[1,2]

Scheme S2. Synthesis of azide-terminated PNIPAM.

Taking azide-terminated $PNIPAM_{22}$ as an example, NIPAM (3.0 g, 26.5 mmol), CuCl (227 mg, 2.27 mmol), Me_6TREN (522 mg, 2.27 mmol) and DMF/water (10 mL, v:v = 1:1) were introduced into a 50 mL Schlenk flask. The flask was degassed by three freeze-pump-thaw cycles and the azide-functionalized initiator (178 mg, 0.75 mmol) was introduced via a gastight syringe to initiate the polymerization. The polymerization lasted 10 h at room temperature and it was terminated by putting the flask into liquid N_2. The solution was passed through a short Al_2O_3 column to remove residual catalyst. The mixture was precipitated into *n*-hexane. The crude product was purified by repeated dissolution in THF and precipitation in *n*-hexane followed by drying *in vacuo* overnight to give azide-terminated PNIPAM as white solid, which was subjected to GPC and ^{1}H NMR analysis. Its 'absolute' molecular weight was determined by ^{1}H NMR after coupling to OPE_7. GPC: M_n^{GPC} = 3,400 g/mol, M_w/M_n = 1.21. ^{1}H NMR (400 MHz, $CDCl_3$): δ (ppm): (4H, $N_3CH_2CH_2OCH_2CH_2O_2C$): 0.80-2.75 (9H, $CH_2CHCONHCH(CH_3)_2$), 3.44 (2H, $N_3CH_2CH_2OCH_2CH_2O_2C$), 3.67 (4H, $N_3CH_2CH_2OCH_2CH_2$), 4.00 (1H, $CH_2CHCONHCH(CH_3)_2$), 4.24 (2H, $N_3CH_2CH_2OCH_2CH_2O_2C$), 6.60-7.00 (1H, $CH_2CHCONHCH(CH_3)_2$).

Synthesis of OPE$_7$-*b*-PNIPAM diblock copolymer

OPE$_7$-*b*-PNIPAM$_{22}$ and OPE$_7$-*b*-PNIPAM$_8$ diblock copolymers were synthesized (**Scheme S3**) and purified in a similar way as described in our previous reports.[1,2] Cu-catalyzed alkyne-azide cycloaddition (CuAAC) reaction ("Click") was used to synthesize OPE$_7$-*b*-PNIPAM$_{22}$ and OPE$_7$-*b*-PNIPAM$_8$ diblock copolymers between alkyne-terminated OPE$_7$ and azide-terminated PNIPAM.

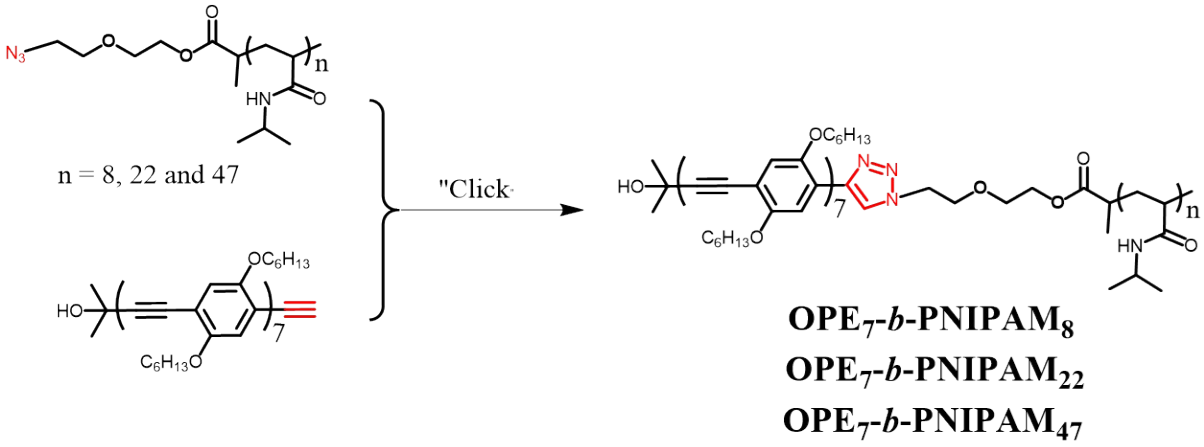

Scheme S3. Synthetic route of OPE$_7$-*b*-PNIPAM diblock copolymers.

Taking OPE$_7$-*b*-PNIPAM$_{22}$ as an example, alkyne-terminated OPE$_7$ (25 mg, 11.4 μmol), PNIPAM$_{22}$ (80 mg, 29.6 μmol), CuCl (3 mg, 30.3 μmol) and TBTA (17 mg, 32.1 μmol) were added into a 25 mL Schlenk flask followed by adding 5 mL of dry THF via a gastight syringe. The flask was degassed by three freeze-pump-thaw cycles followed by immersing the flask into an oil bath set at 50°C. The reaction mixture was allowed to stir for 24 h. The solvent was evaporated and the residue was purified by silica column chromatography (eluent: CH_2Cl_2/ethyl acetate = 10/1) to remove the unreacted OPE$_7$. To remove excess PNIPAM$_{22}$, the crude product was purified by repeated dissolution in THF and precipitation in water/ ethanol (v/v = 1/1) three times, followed by drying *in vacuo* overnight to give 42 mg (75%) of OPE$_7$-*b*-PNIPAM$_{22}$ diblock copolymer as yellow solid. The number-average degree of

polymerization of PNIPAM block was determined by ^{1}H NMR on the basis of known DP_n of alkyne-terminated OPE_7. GPC: M_n^{GPC} = 7200 g/mol, M_w/M_n = 1.06.

Self-assembly Experiments

Self-assembly of OPE_7-*b*-PNIPAM diblock copolymers

A concentrated THF solution (10 mg/mL) of OPE_7-*b*-$PNIPAM_n$ (n = 8, 22 and 47) was added into hot (80°C) ethanol, ethanol/water (v/v = 90/10, 80/20 and 75/25) until the concentration reached 0.05 mg/mL. Subsequently, the solution was heated at 80°C for 30 min, followed by cooling in air and aging at room temperature (23°C) for 24 h. A drop of resulting solution was placed on a Formvar and carbon-coated copper grid and examined by TEM.

Preparation of seed micelles

Seed micelles were prepared by sonicating (SONICS VC 750 ultrasonic processor, 30% power) the corresponding polydisperse micelles of OPE_7-*b*-$PNIPAM_n$ (for n = 8 and 47, 0.05 mg/mL in ethanol/H_2O, v/v = 90/10; for n = 22, 0.05 mg/mL in ethanol/H_2O, v/v = 95/5, 90/10, 80/20 and 75/25) at 0°C for 30 min. A drop of fresh seed solution or seed solution after aging at room temperature (23°C) for 24 h was placed on a Formvar and carbon-coated copper grid and examined by TEM.

Self-seeding of OPE_7-*b*-$PNIPAM_n$

Self-seeding of OPE_7-*b*-$PNIPAM_n$ (n = 8 and 47) was conducted by thermal annealing

corresponding seed micelles at different temperatures. Aliquots of seed micellar solution in several vials (0.4 mL/vial) were put into water-baths set at different temperatures and heated for 30 min, followed by cooling in air and aging at room temperature (23°C) for 24 h. Finally, a drop of each solution was placed on a Formvar and carbon-coated copper grid and examined by TEM.

SUPPORTING FIGURES

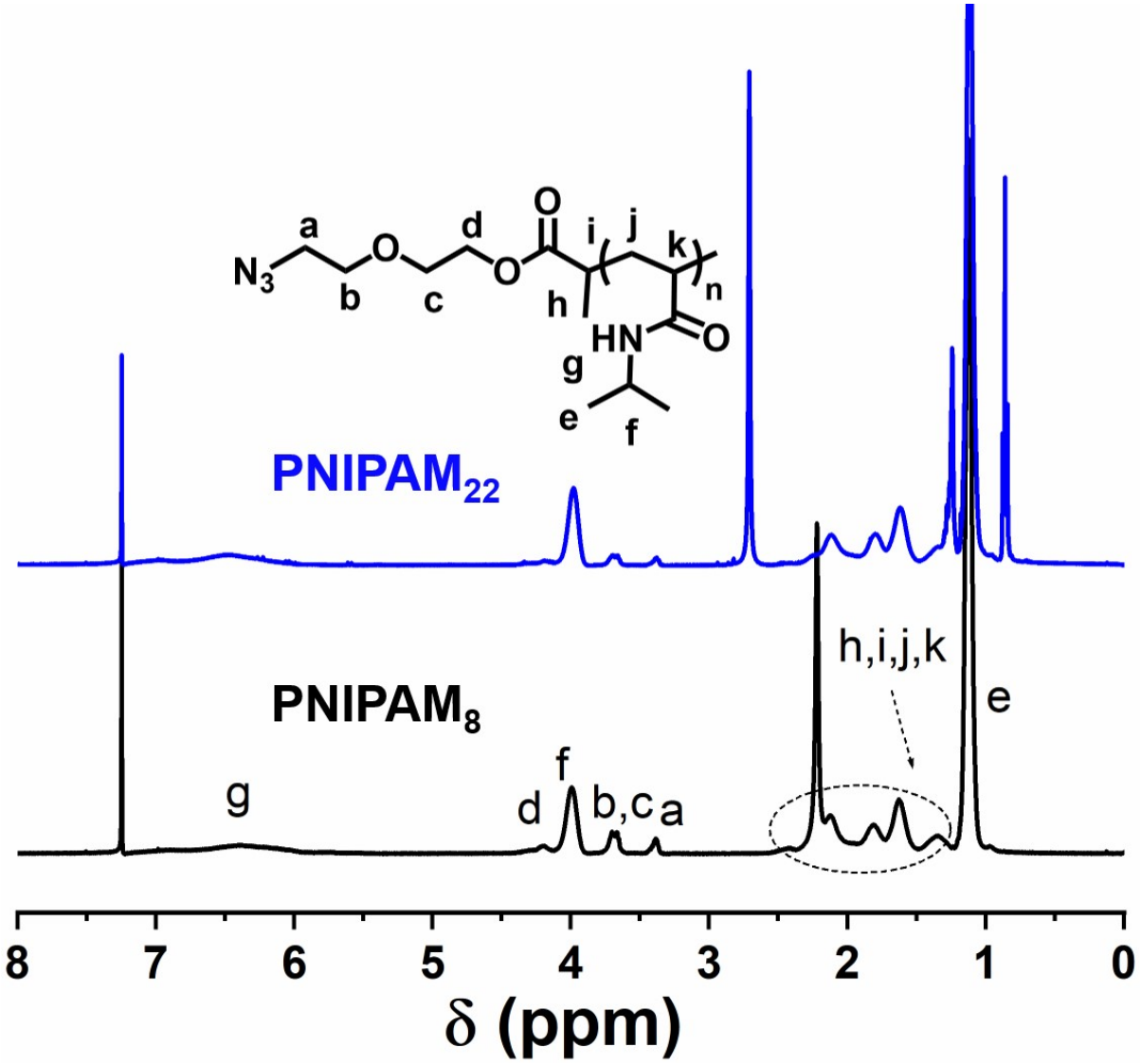

Figure S1. ^{1}H NMR spectra of azide-terminated $PNIPAM_8$ and $PNIPAM_{22}$ in $CDCl_3$.

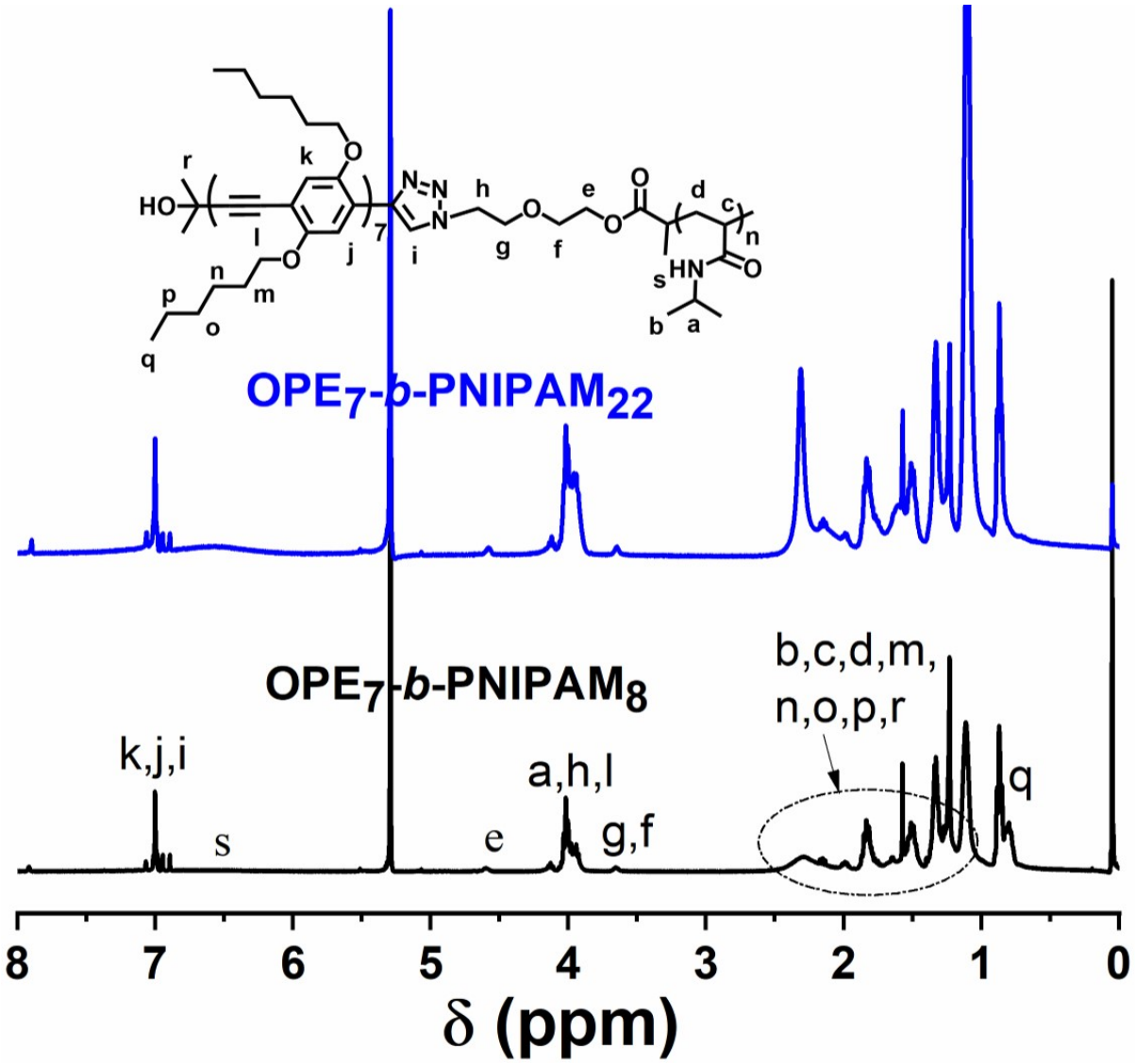

Figure S2. ^{1}H NMR spectra of OPE_7-*b*-$PNIPAM_8$ and OPE_7-*b*-$PNIPAM_{22}$ in CD_2Cl_2.

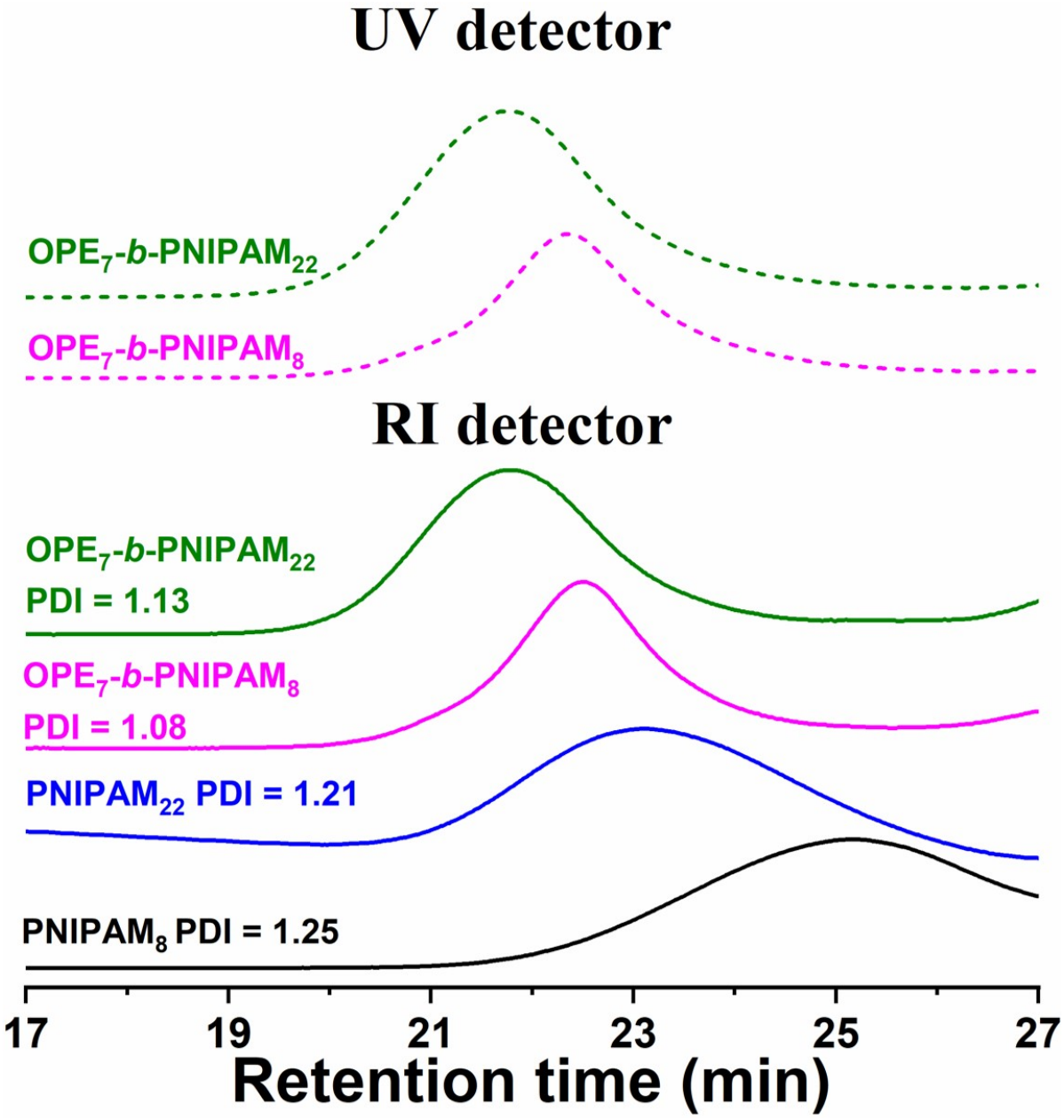

Figure S3. GPC curves of azide-terminated $PNIPAM_8$ and $PNIPAM_{22}$, OPE_7-*b*-$PNIPAM_8$ and OPE_7-*b*-$PNIPAM_{22}$ in THF.

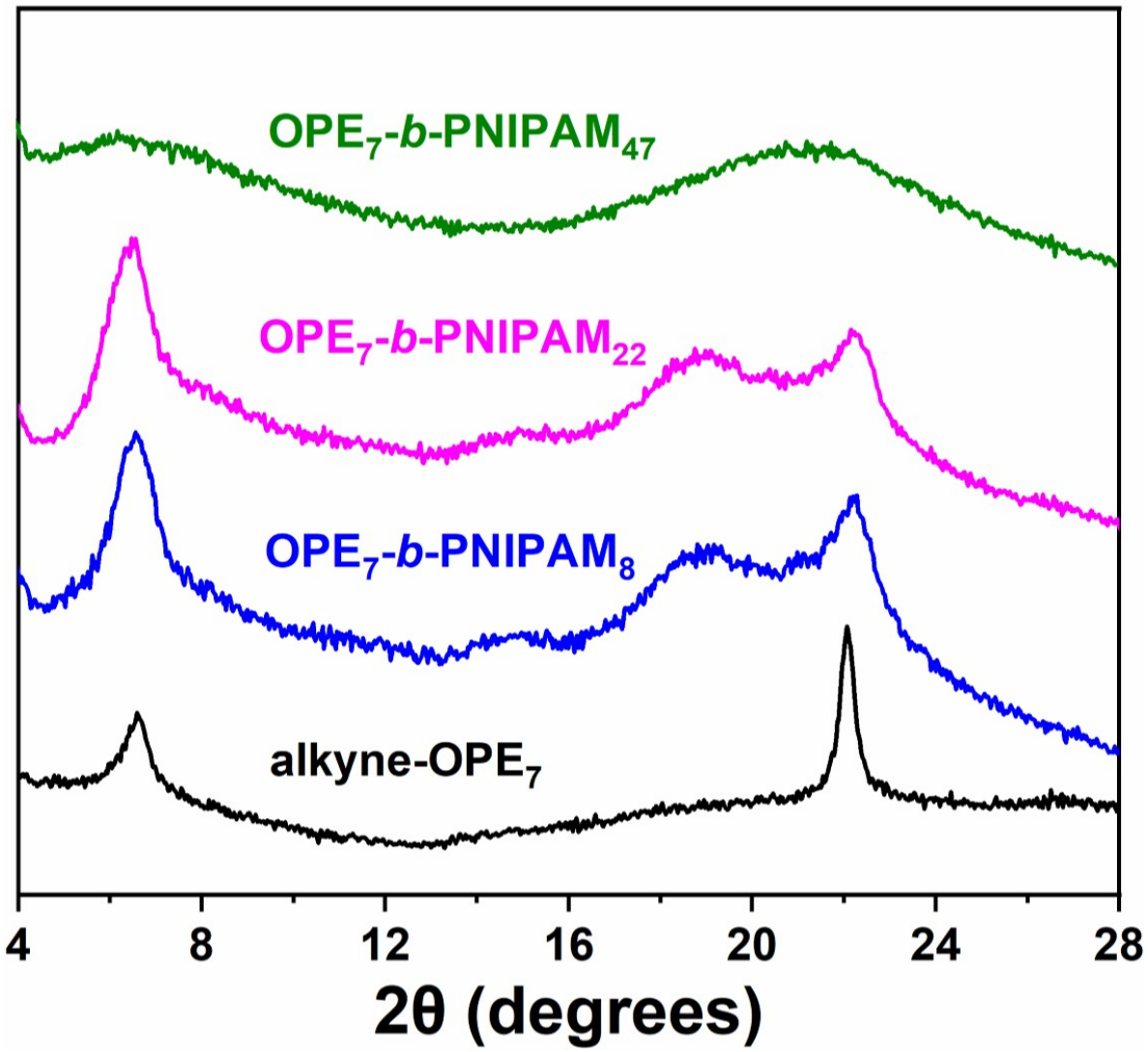

Figure S4. XRD patterns of alkyne-terminated OPE_7, OPE_7-*b*-$PNIPAM_8$, OPE_7-*b*-$PNIPAM_{22}$ and OPE_7-*b*-$PNIPAM_{47}$.

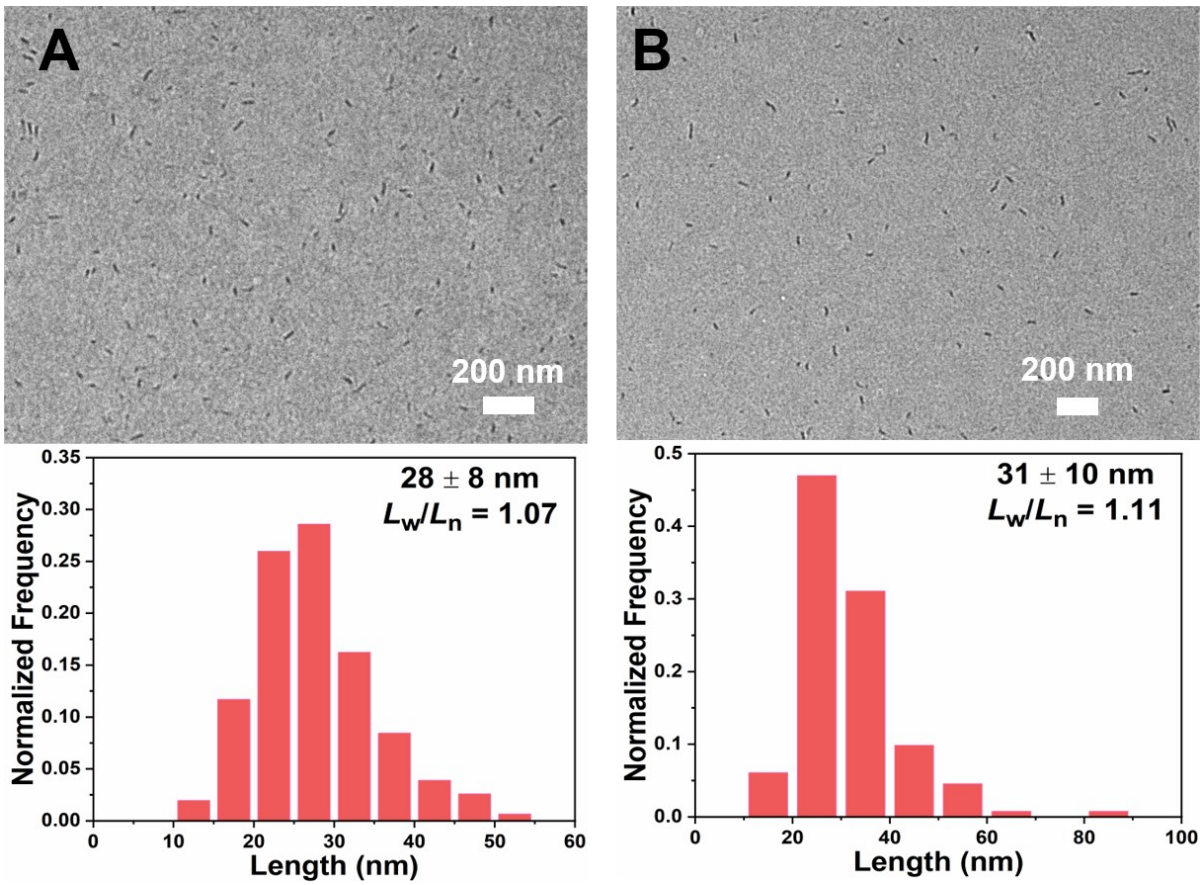

Figure S5. TEM images and histograms of length distribution of seed micelles of OPE_7-*b*-$PNIPAM_{22}$ (0.05 mg/mL in ethanol) before (A) and after (B) storing at -18 ℃ for 24 h.

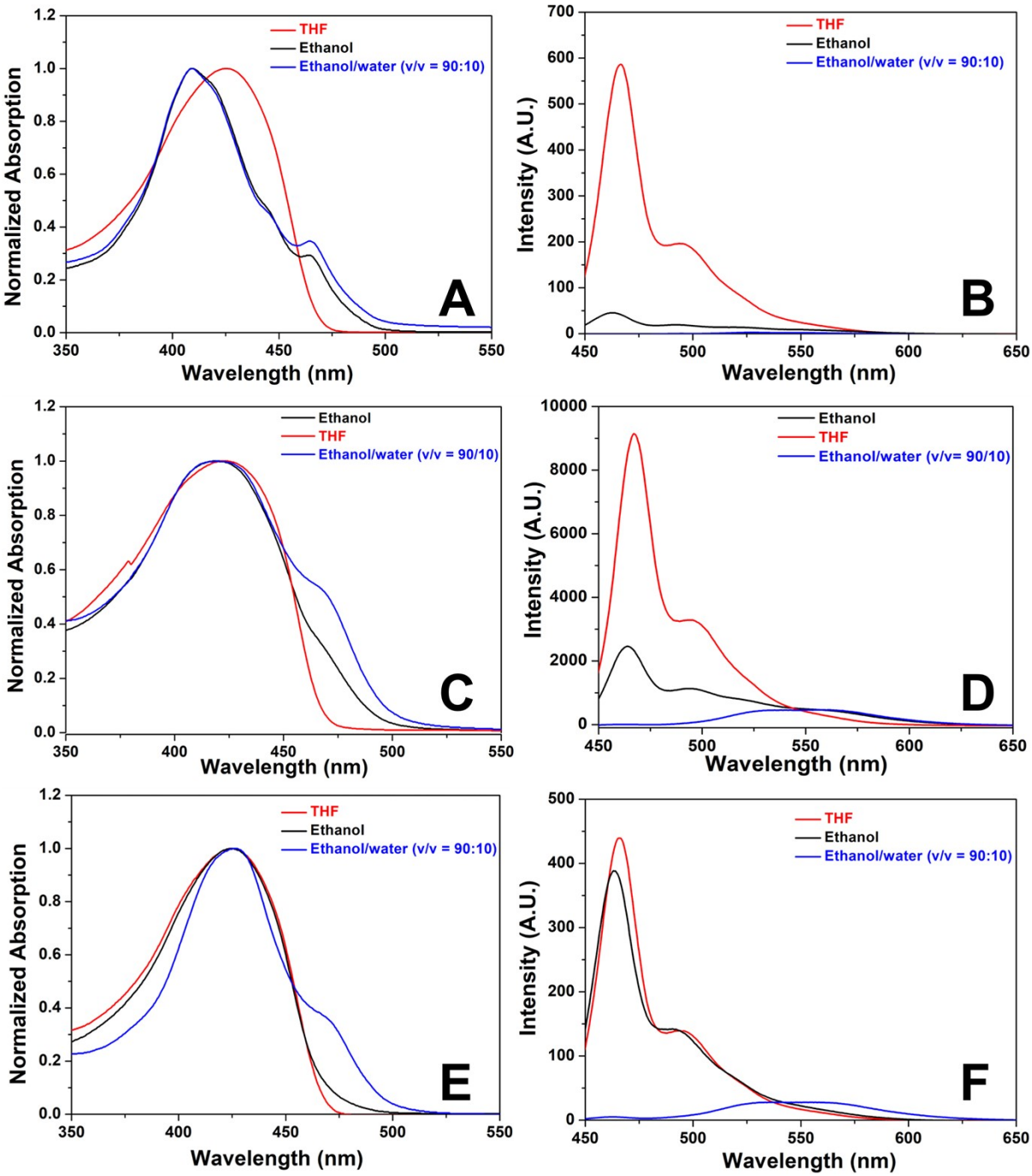

Figure S6. (A) UV/vis absorption and (B) fluorescence spectra of OPE_7-*b*- $PNIPAM_8$ in THF, ethanol and ethanol/water (v/v = 9/1) with a concentration of 0.05 mg/mL. (C) UV/vis absorption and (D) fluorescence spectra of OPE_7-*b*-$PNIPAM_{22}$ in THF, ethanol and ethanol/ water (v/v = 9/1) with a concentration of 0.05 mg/mL. (E) UV/vis absorption and (F) fluorescence spectra of OPE_7-*b*-$PNIPAM_{47}$ in THF, ethanol and ethanol/water (v/v = 9/1) with a concentration of 0.05 mg/mL.

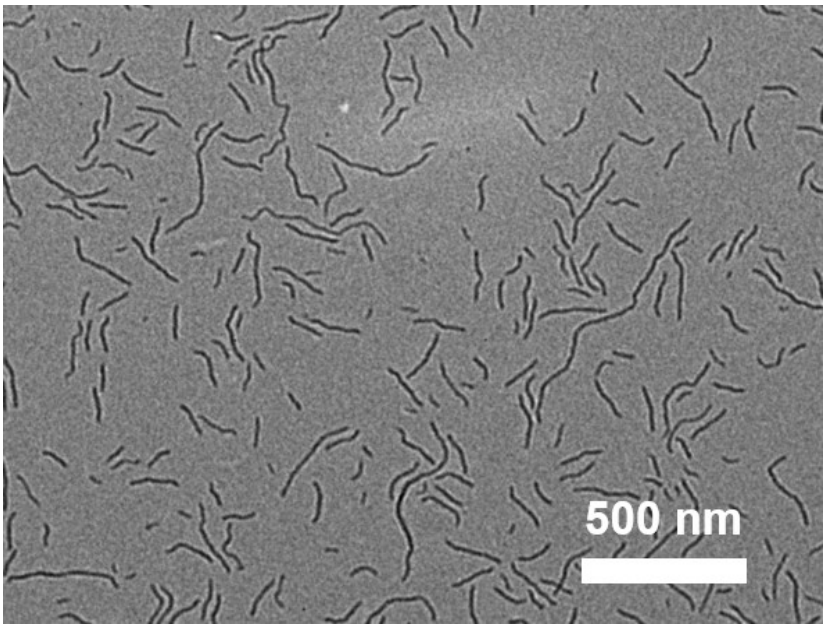

Figure S7. TEM image of micelles of OPE_7-*b*-$PNIPAM_{22}$ (0.05 mg/mL in ethanol/H_2O, v/v = 75/25) formed by heating/cooling process.

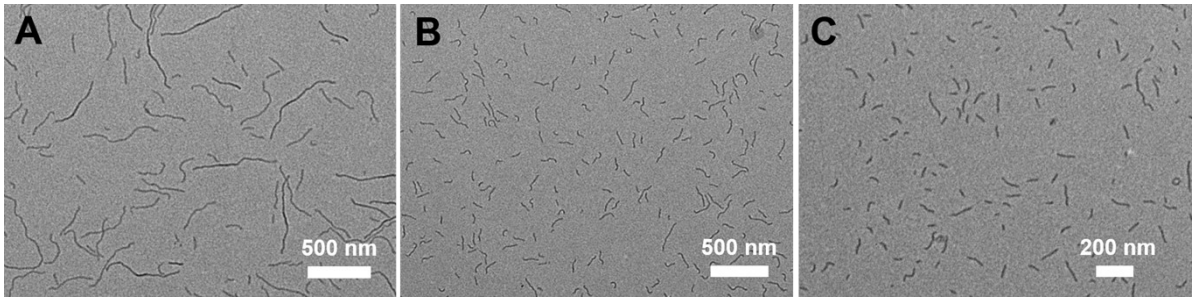

Figure S8. TEM images of micelles of OPE_7-*b*-$PNIPAM_{47}$ (0.05 mg/mL) in the mixture of ethanol/H_2O with v/v = (A) 80/20, (B) 75/25 and (C) 70/30, respectively, formed by heating/ cooling process.

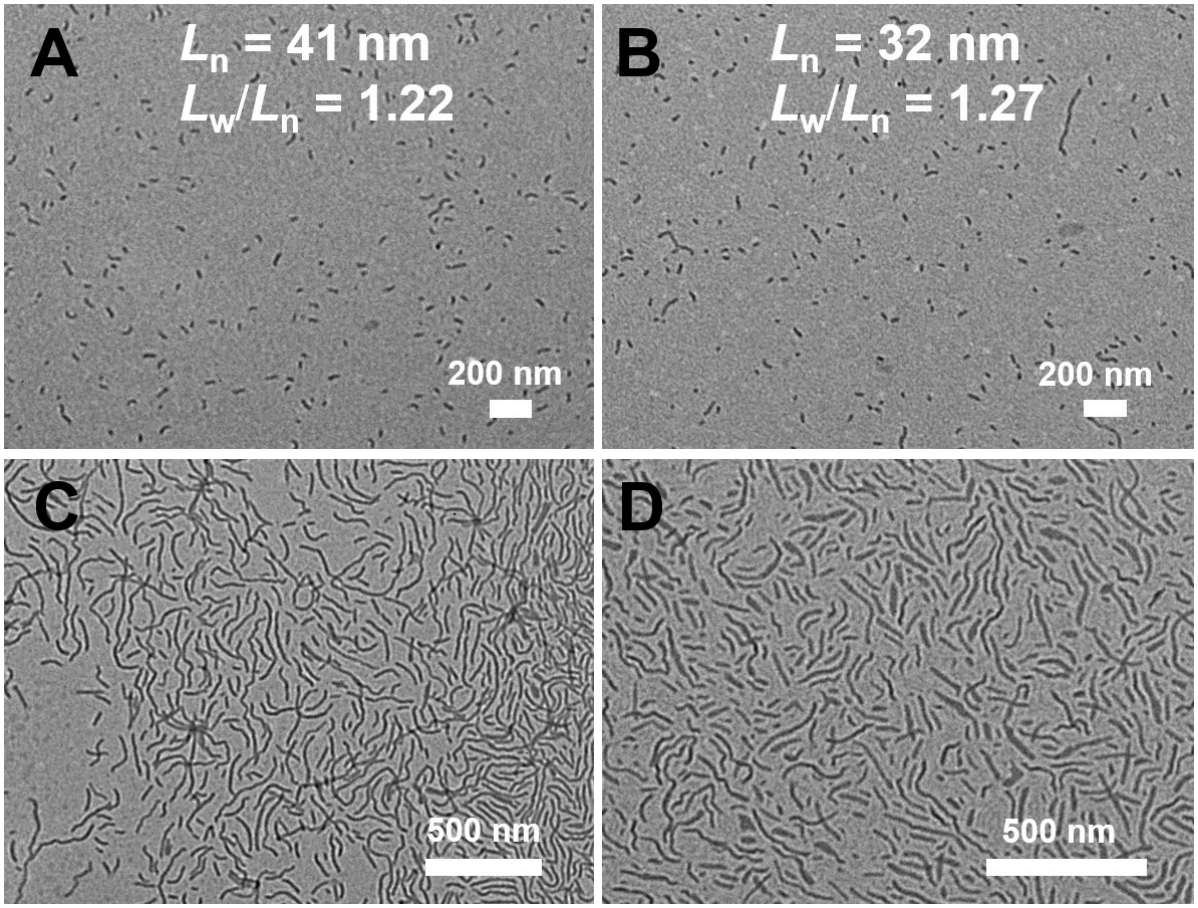

Figure S9. TEM images of micelles of OPE_7-*b*-$PNIPAM_{47}$ formed in ethanol/H_2O with (A) 35 and (B) 40 v/v of water and micelles of OPE_7-*b*-$PNIPAM_{22}$ formed in ethanol/H_2O with (C) 35 and (D) 40 v/v of water.

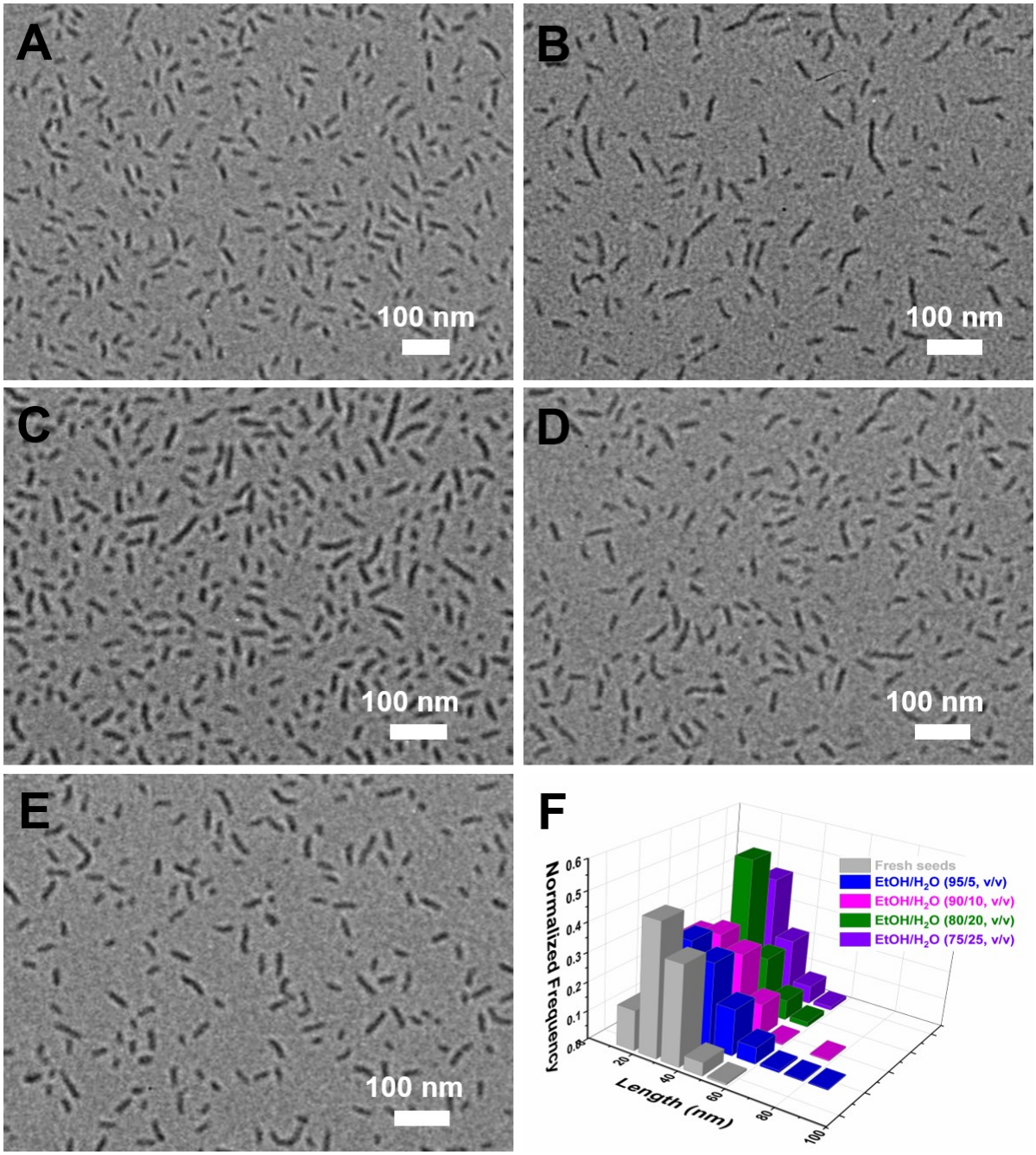

Figure S10. TEM images of (A) initial mother seed micelles of OPE_7-*b*-$PNIPAM_{22}$ in ethanol/water (0.1 mg/mL, v/v = 90/10) and diluted seed micelles in ethanol/water (0.05 mg/mL) with v/v = (B) 95/5, (C) 90/10, (D) 80/20 and (E) 75/25, respectively, after storing at room temperature for 24 h. (F) Histograms of length distribution of corresponding seed micelles as shown in panels A-E.

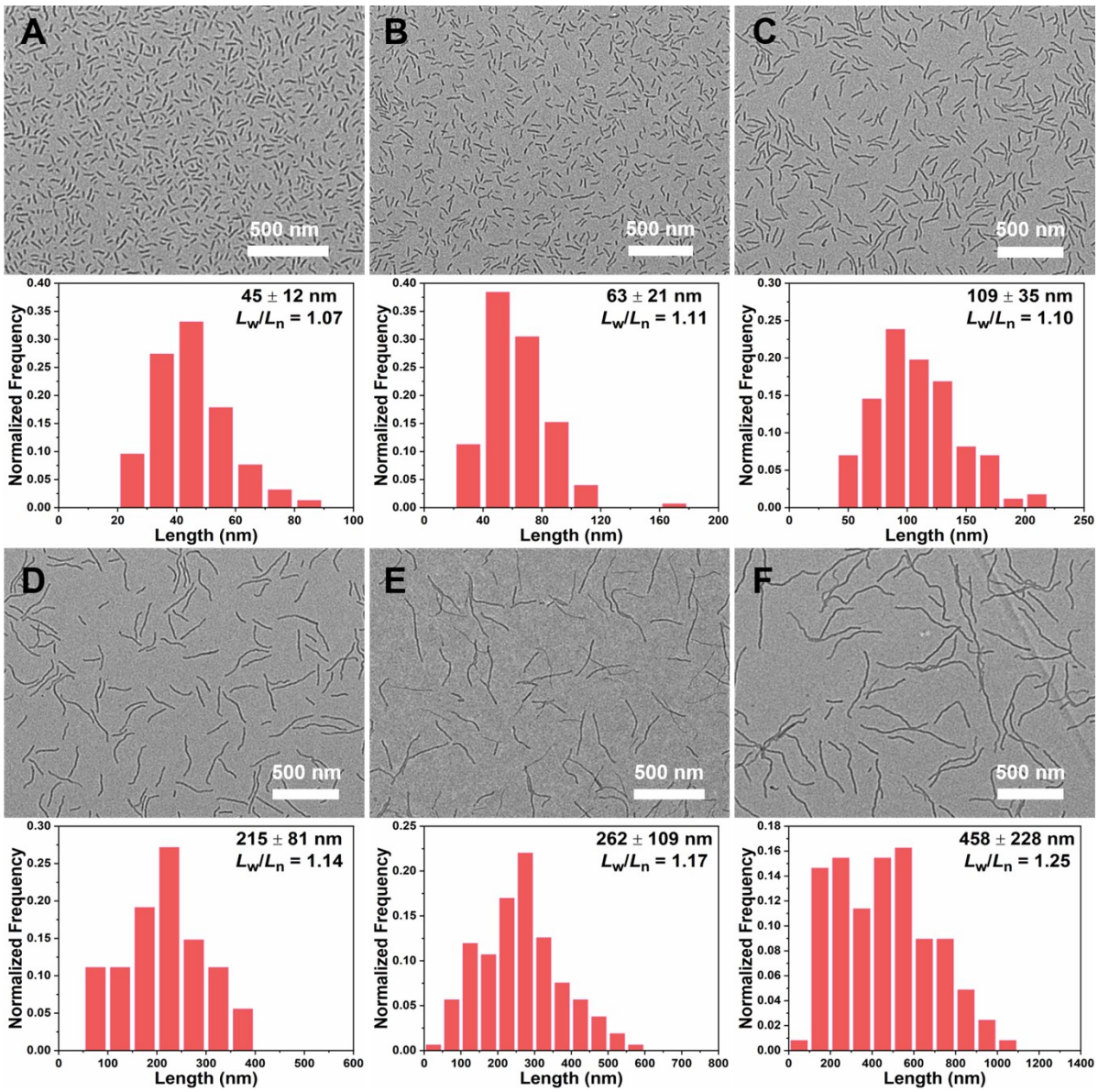

Figure S11. TEM images and histograms of length distribution of fiber-like micelles of OPE_7-*b*-$PNIPAM_{22}$ obtained by annealing the seeds at (A) 45°C, (B) 50°C, (C) 55°C, (D) 58°C, (E) 60°C and (F) 62°C in ethanol/water (0.05 mg/mL, 90/10, v/v) and cooling/aging at room temperature for 24 h.

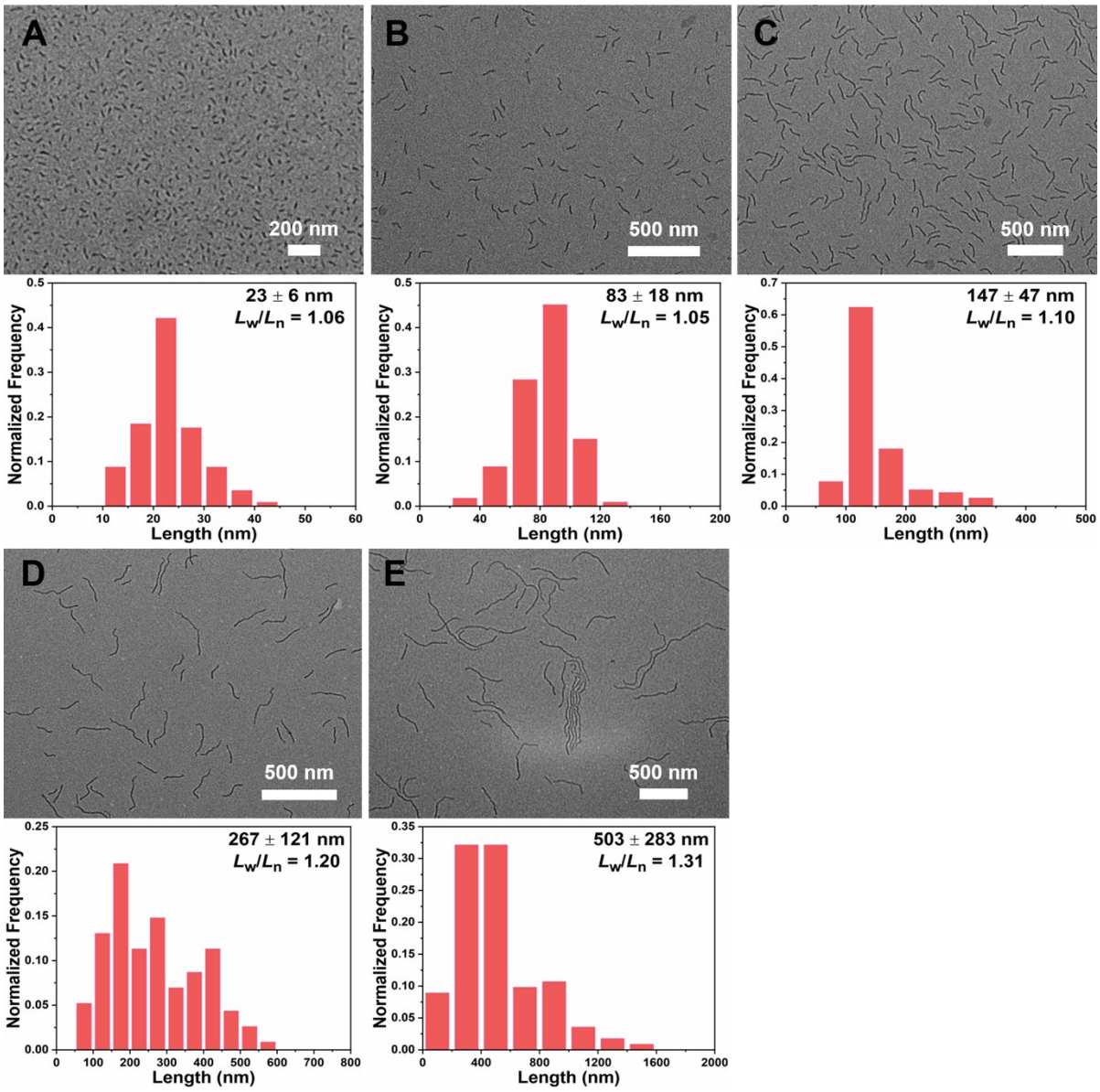

Figure S12. TEM images and histograms of length distribution of (A) seed micelles and fiber-like micelles of OPE_7-*b*-$PNIPAM_{47}$ obtained by annealing the seeds at (B) 45°C, (C) 50°C, (D) 52°C and (E) 55°C in ethanol/water (0.05 mg/mL, 90/10, v/v) and cooling/aging at room temperature for 24 h.

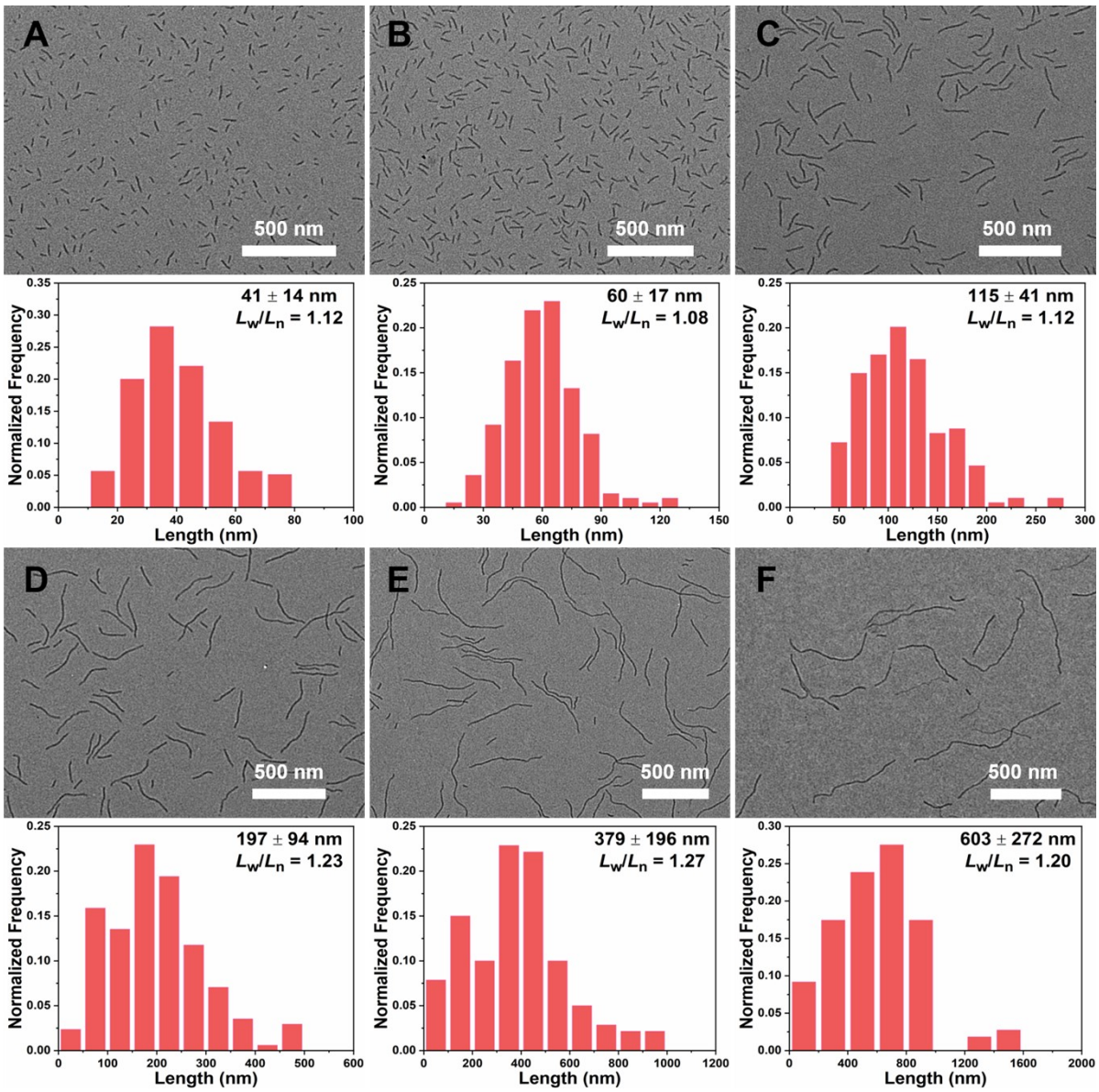

Figure S13. TEM images and histograms of length distribution of fiber-like micelles of OPE_7-*b*-$PNIPAM_{22}$ obtained by annealing the seeds at (A) 30°C, (B) 40°C, (C) 45°C, (D) 48°C, (E) 50°C and (F) 52°C in ethanol/water (0.05 mg/mL, 95/5, v/v) and cooling/aging at room temperature for 24 h.

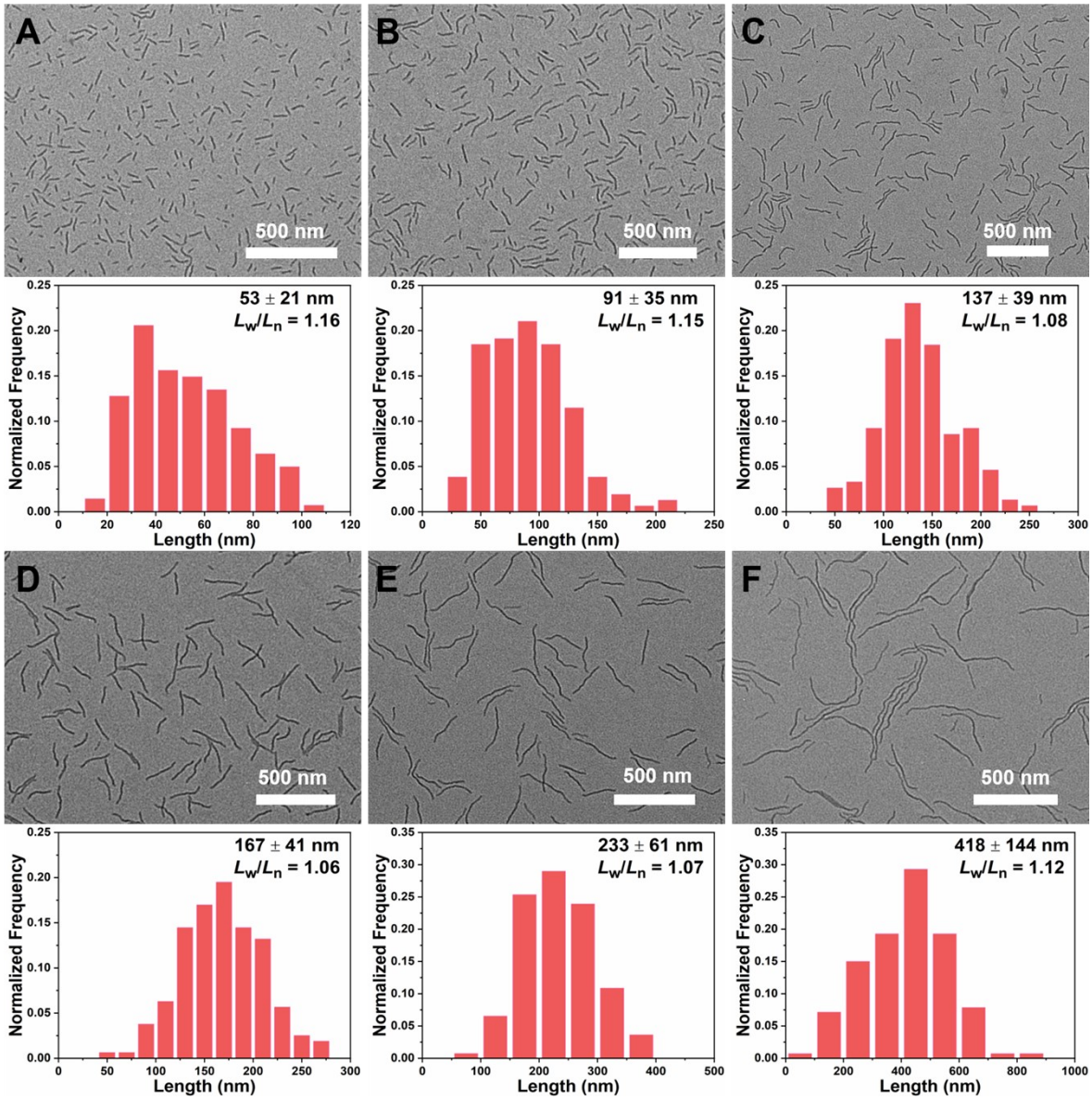

Figure S14. TEM images and histograms of length distribution of fiber-like micelles of OPE_7-*b*-$PNIPAM_{22}$ obtained by annealing the seeds at (A) 60°C, (B) 70°C, (C) 75°C, (D) 77°C, (E) 79°C and (F) 81°C in ethanol/water (0.05 mg/mL, 80/20, v/v) and cooling/aging at room temperature for 24 h.

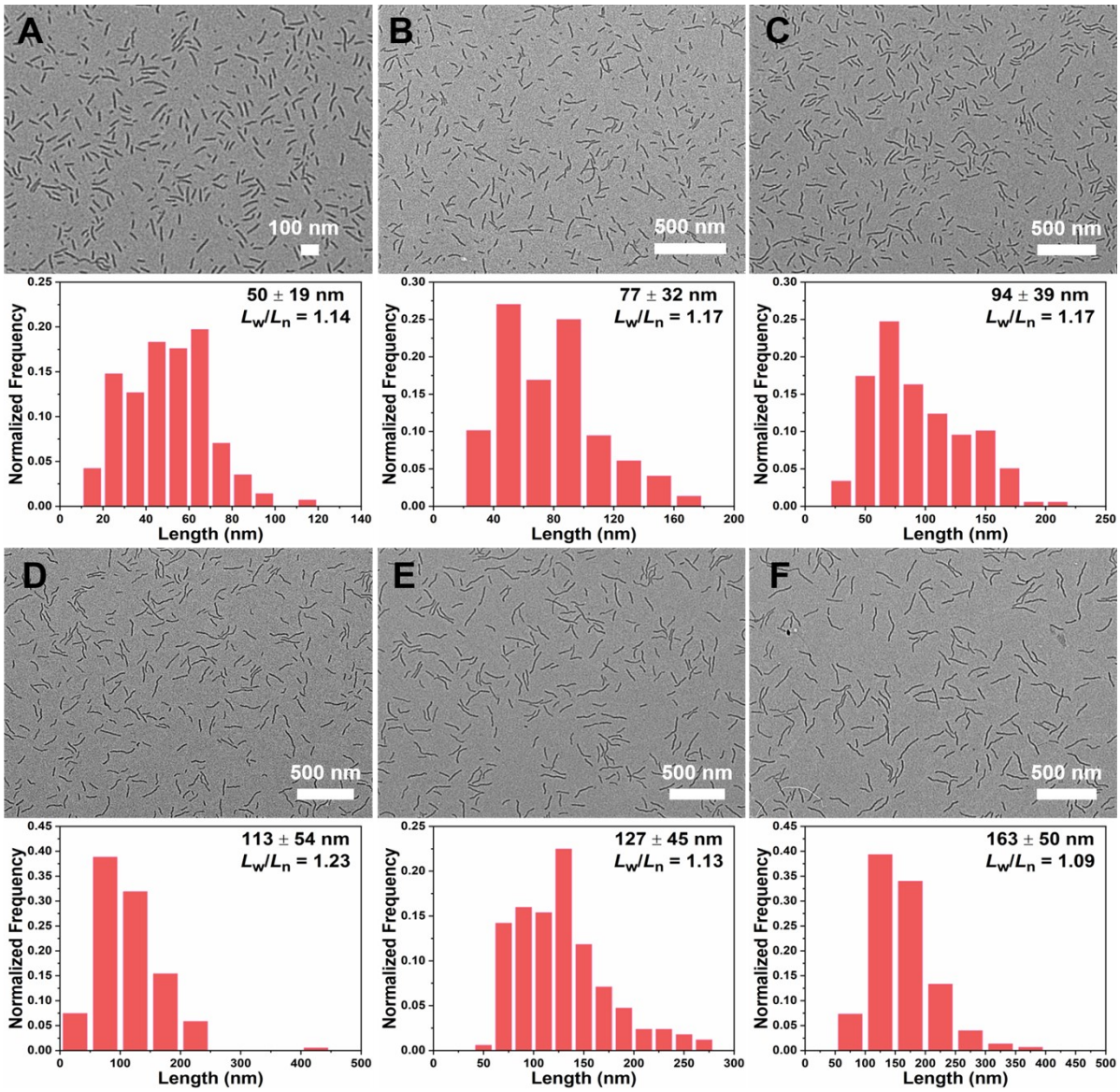

Figure S15. TEM images and histograms of length distribution of fiber-like micelles of OPE_7-*b*-$PNIPAM_{22}$ obtained by annealing the seeds at (A) 60℃, (B) 70℃, (C) 75℃, (D) 80℃, (E) 83℃ and (F) 85℃ in ethanol/water (0.05 mg/mL, 75/25, v/v) and cooling/aging at room temperature for 24 h.

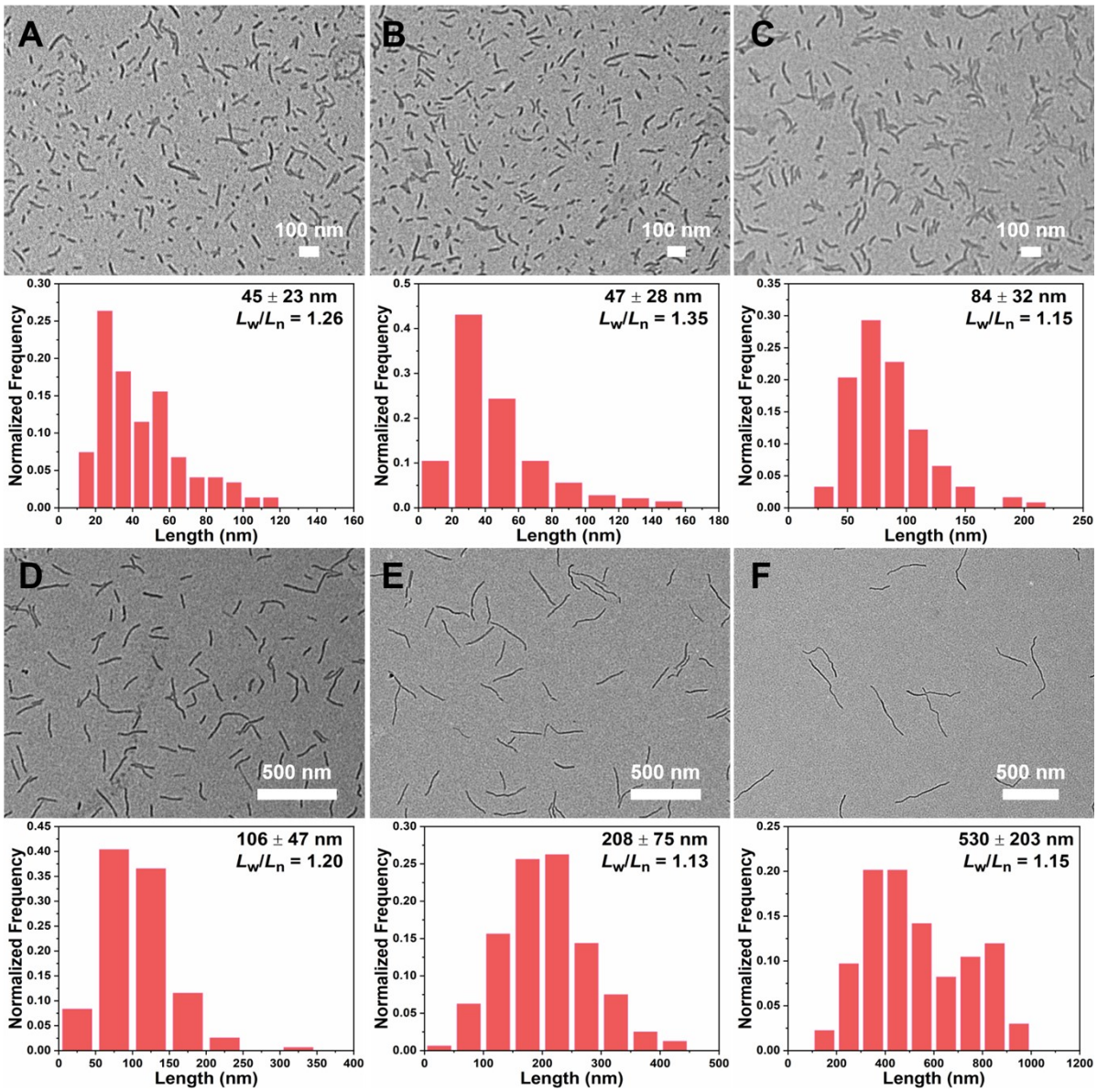

Figure S16. TEM images and histograms of length distribution of seeds (A) before and (B) after storing at room temperature for 2 days and fiber-like micelles of OPE_7-*b*-$PNIPAM_{22}$ obtained by annealing the seeds at (C) 45°C, (D) 50°C, (E) 55°C and (F) 57°C in methanol (0.05 mg/mL) and cooling/aging at room temperature for 24 h.

SUPPORTING TABLES

Table S1. Characteristics of seed micelle before and after storing in ethanol at -18℃ for 24 h[a]

T (°C)	L_n (nm)	L_w (nm)	L_w/L_n[b]	σ[b] (nm)	σ/L_n[b]
Initial seed	28	30	1.07	8	0.27
-18℃	31	35	1.11	10	0.33

[a] The mean length of micelles was calculated from measurements of over 100 individual micelles in multiple TEM images.

[b] L_n, L_w and σ are number-average micelle length, weight-average micelle length and standard deviation of micelle length distribution, respectively, as calculated from the histogram of length distribution.

Table S2. Characteristics of seed and elongated micelles of OPE_7-*b*-$PNIPAM_{22}$ obtained by annealing the seeds in ethanol/water (90/10, v/v) at different temperatures and then cooling/aging at room temperature[a]

T (°C)	L_n (nm)	L_w (nm)	L_w/L_n[b]	σ[b] (nm)	$σ/L_n$[b]
seed	27	31	1.14	10	0.37
45	45	49	1.07	12	0.27
50	63	70	1.11	21	0.33
55	109	120	1.10	35	0.32
58	215	246	1.14	81	0.38
60	262	307	1.17	109	0.41
62	458	571	1.25	228	0.50

[a] The mean length of micelles was calculated from measurements of over 100 individual micelles in multiple TEM images.

[b] L_n, L_w and σ are number-average micelle length, weight-average micelle length and standard deviation of micelle length distribution, respectively, as calculated from the histogram of length distribution.

Table S3. Characteristics of seed micelles and elongated micelles of OPE_7-*b*-$PNIPAM_{47}$ obtained by annealing the seeds in ethanol/water (90/10, v/v) at different temperatures and then cooling/aging at room temperature[a]

T (°C)	L_n (nm)	L_w (nm)	L_w/L_n[b]	σ[b] (nm)	$σ/L_n$[b]
seed	23	25	1.06	6	0.25
45	83	86	1.05	18	0.21
50	147	162	1.10	47	0.32
52	267	321	1.20	121	0.45
55	503	661	1.31	283	0.56

[a] The mean length of micelles was calculated from measurements of over 100 individual micelles in multiple TEM images.

[b] L_n, L_w and σ are number-average micelle length, weight-average micelle length and standard deviation of micelle length distribution, respectively, as calculated from the histogram of length distribution.

Table S4. Characteristics of seed and elongated micelles of OPE_7-*b*-$PNIPAM_{22}$ obtained by annealing the seeds in ethanol/water (95/5, v/v) at different temperatures and then cooling/aging at room temperature[a]

T (°C)	L_n (nm)	L_w (nm)	L_w/L_n[b]	σ[b] (nm)	$σ/L_n$[b]
seed	33	38	1.15	13	0.39
35	41	46	1.12	14	0.35
40	60	65	1.08	17	0.29
45	115	130	1.12	41	0.35
48	197	242	1.23	94	0.48
50	379	480	1.27	196	0.52
52	603	725	1.20	272	0.45

[a] The mean length of micelles was calculated from measurements of over 100 individual micelles in multiple TEM images.

[b] L_n, L_w and σ are number-average micelle length, weight-average micelle length and standard deviation of micelle length distribution, respectively, as calculated from the histogram of length distribution.

Table S5. Characteristics of seed and elongated micelles of OPE_7-*b*-$PNIPAM_{22}$ obtained by annealing the seeds in ethanol/water (80/20, v/v) at different temperatures and then cooling/aging at room temperature[a]

T (°C)	L_n (nm)	L_w (nm)	L_w/L_n[b]	σ[b] (nm)	$σ/L_n$[b]
seed	27	29	1.09	8	0.30
60	53	61	1.16	21	0.40
70	91	105	1.15	35	0.39
75	137	148	1.08	39	0.28
77	167	177	1.06	41	0.25
79	233	249	1.07	61	0.26
81	418	467	1.12	144	0.34

[a] The mean length of micelles was calculated from measurements of over 100 individual micelles in multiple TEM images.

[b] L_n, L_w and σ are number-average micelle length, weight-average micelle length and standard deviation of micelle length distribution, respectively, as calculated from the histogram of length distribution.

Table S6. Characteristics of seed and elongated micelles of OPE_7-*b*-$PNIPAM_{22}$ obtained by annealing the seeds in ethanol/water (75/25, v/v) at different temperatures and then cooling/aging at room temperature[a]

T (°C)	L_n (nm)	L_w (nm)	L_w/L_n[b]	σ[b] (nm)	$σ/L_n$[b]
seed	26	29	1.12	9	0.35
60	50	57	1.14	19	0.38
70	77	91	1.17	32	0.42
75	94	110	1.17	39	0.41
80	113	139	1.23	54	0.48
83	127	143	1.13	45	0.36
85	163	178	1.09	50	0.31

[a] The mean length of micelles was calculated from measurements of over 100 individual micelles in multiple TEM images.

[b] L_n, L_w and σ are number-average micelle length, weight-average micelle length and standard deviation of micelle length distribution, respectively, as calculated from the histogram of length distribution.

Table S7. Characteristics of seed and elongated micelles of OPE_7-*b*-$PNIPAM_{22}$ obtained by annealing the seeds in methanol at different temperatures and then cooling/aging at room temperature[a]

T (°C)	L_n (nm)	L_w (nm)	L_w/L_n[b]	σ[b] (nm)	$σ/L_n$[b]
seed	45	57	1.26	23	0.51
seed/2d	47	63	1.35	28	0.59
45	84	96	1.15	32	0.39
50	106	127	1.20	47	0.44
55	208	235	1.13	75	0.36
57	530	607	1.15	203	0.38

[a] The mean length of micelles was calculated from measurements of over 100 individual micelles in multiple TEM images.

[b] L_n, L_w and σ are number-average micelle length, weight-average micelle length and standard deviation of micelle length distribution, respectively, as calculated from the histogram of length distribution.

References and Notes

1. Nie, J. C.; Wang, Z. Q.; Huang, X. Y.; Lu, G. L.; Feng, C. Uniform continuous and segmented nanofibers containing a π-conjugated oligo(*p*-phenylene ethynylene) core via "living" crystallization-driven self-assembly: importance of oligo(*p*-phenylene ethynylene) chain length. *Macromolecules* **2020**, *53*, 6299-6313.

2. Nie, J. C.; Huang, X. Y.; Lu, G. L.; Winnik, M. A.; Feng, C. Synthesis and living crystallization-driven self-assembly of backbone asymmetric and symmetric π-conjugated oligo(*p*-phenylene ethynylene)-based block copolymers. *Polym. Chem.* **2023**, *14*, 137-151.